

Investigating the Molecular Mechanisms of Prostate Cancer Bone Metastasis

Ella Yee, Florencia Picech, Cory Abate-Shen

Abstract

Metastasis is the leading cause of death in prostate cancer, which is estimated to cause 35,770 deaths in the United States in 2025. Metastasis to the bone, the most common site, is associated with lower survival rates and health complications such as severe pain, fractures, and spinal cord compression due to the formation of osteoblastic lesions. With limited knowledge of the intrinsic and extrinsic mechanisms of bone metastasis, current treatments target the bone remodelling process rather than primary tumors and thus are not curative. To address this limitation, we performed histopathological analyses of primary tumors and matched metastases to the lung, liver and bone in genetically engineered mouse models of advanced prostate cancer. In particular, the expression of androgen receptor (AR), vimentin (VIM), and cytokeratins (PanCK) were compared between NPK (*Nkx3.1*^{CreERT2/+}; *Pten*^{flox/flox}; *Kras*^{LSL-G12D/+}; *R26R-CAG*^{LSL-EYFP/+}) and NPp53Rb1^{+/−} (*Nkx3.1*^{CreERT2/+}; *Rb1*^{flox/+}; *Pten*^{flox/flox}, *p53*^{flox/flox}; *R26R-CAG*^{LSL-EYFP/+}) genotypes to evaluate the contributions of AR signaling and epithelial-mesenchymal transition (EMT) to metastatic progression. In both genotypes, the molecular phenotypes of metastatic sites corresponded to those of their primary tumors. NPK mice exhibited positive expression of AR, VIM, and PanCK in both primary and metastatic lesions, consistent with active AR signaling and EMT. In contrast, NPp53Rb1^{+/−} mice did not express AR, VIM, or PanCK. These findings suggest that the intrinsic features of primary tumors are retained during metastatic progression and may determine the mechanisms of metastasis to sites including bone. Furthermore, the differing expression profiles of NPK and NPp53Rb1^{+/−} mice, despite both genotypes developing high incidences of bone metastases, supports the existence of distinct mechanisms of bone metastasis among disease subtypes, highlighting the importance of subtype-specific approaches to treating prostate cancer.

I. Introduction

Prostate cancer is the most commonly diagnosed cancer among men in the United States and is projected to cause approximately 35,770 deaths in 2025 (Siegel *et al.* 2025). While localized prostate tumors are typically indolent and treatable, advanced forms of the disease can be aggressive and ultimately fatal. Because androgens promote the growth of prostate cells through the androgen receptor (AR) signaling pathway, the standard treatment for advanced prostate cancer is androgen deprivation therapy via surgical or chemical castration. However, many patients eventually develop castration-resistant prostate cancer (CRPC), which is often highly metastatic. In some cases, metastasis can also arise de novo. CRPC and de novo metastatic prostate cancer are associated with poor prognosis and limited treatment options (Rebello *et al.* 2021).

Metastasis is the leading cause of death among prostate cancer patients, with bone being the most frequent site (Arriaga *et al.* 2020). Bone metastasis is facilitated by complex interactions between prostate cancer cells and the bone microenvironment, although the precise mechanisms driving this process remain unclear. Three major cell types comprising the bone microenvironment are osteocytes, osteoblasts, and osteoclasts. Osteocytes regulate the activity of osteoblasts and osteoclasts. Osteoblasts contribute to bone formation, while osteoclasts contribute to bone resorption (Wang *et al.* 2019). Prostate cancer bone metastases are typically osteoblastic in nature, characterized by excessive bone formation. These lesions can cause severe pain, fractures, spinal cord compression, and other health complications that significantly compromise patient quality of life. While treatments such as monoclonal antibodies, bone morphogenic agents, and radiotherapy have been developed to address bone metastases, they target the bone remodeling process rather than the primary tumor. As a result, these therapies are palliative rather than curative (Baldessari *et al.* 2023). Limited knowledge about the intrinsic and extrinsic mechanisms underlying prostate cancer bone metastasis remains a critical barrier to the development of effective treatments.

In addition, a general challenge in studying and treating prostate cancer is disease heterogeneity. Primary tumors of prostate cancer can be categorized into several histological subtypes: Adenocarcinoma is the most common, while rare subtypes such as neuroendocrine prostate cancer may arise through treatment resistance or lineage plasticity (Marra *et al.* 2023). As such, it is critical to investigate how the biological processes driving bone metastasis may differ across subtypes. Two biological processes relevant to this study are AR signaling and the epithelial-mesenchymal transition (EMT). Androgen signaling is triggered when circulating free testosterone enters prostate cells. Testosterone production is regulated by luteinizing hormone (LH), which is regulated by gonadotropin-releasing hormone (GnRH). Within the cytoplasm of prostate cells, testosterone is converted by 5 α -reductase into dihydrotestosterone (DHT), which binds to AR and enables AR translocation into the nucleus. AR then forms dimers that bind to Androgen Response Elements (AREs) found in the promoter and enhancer regions of prostate-specific antigen (PSA), transmembrane protease serine 2 (TMPRSS), and other target genes. The transcription of these target genes contributes to cell proliferation, differentiation, and survival. When dysregulated, for instance by AR overexpression, AR signaling can contribute to the uncontrolled growth of prostate tumor cells (Marra *et al.* 2023). Subtype-specific differences in AR signaling activity can be evaluated through expression of the AR protein. Because prostate adenocarcinomas depend on the AR pathway for growth and survival, they are often responsive to androgen deprivation therapy. In contrast, other subtypes of prostate cancer such as the neuroendocrine phenotype can survive regardless of AR function (Fujita and Nonomura 2019).

Furthermore, EMT is a process by which epithelial cells in the prostate gradually develop mesenchymal features (Figure 1). The dissolution of cell-cell junctions such as desmosomes, adherens junctions, and tight junctions results in decreased cell-to-cell adhesion. Concurrently, weakening of hemidesmosomes and integrins allows cells to detach from the basement membrane. At the molecular level, cells undergoing EMT show decreased expression of epithelial markers such as E-cadherin, occludin, and ZO-1 and increased expression of mesenchymal markers such as fibronectin, N-cadherin, and vimentin. As the mesenchymal phenotype has enhanced invasion and motility capabilities, EMT has been implicated in metastasis. In prostate cancer, EMT is regulated by transcription factors *SNAII/2*, *ZEB1*, *TWIST1*, and *ETS*, which act downstream of signaling pathways such as transforming growth factor (TGF), hepatocyte growth factor (HGF), Wnt/β-catenin, and Notch pathways. (Mittal 2018). Analyzing the expression of cytokeratins (PanCK) and vimentin (VIM) in primary tumors will provide insights into the status of EMT in different tumors, as cytokeratins are markers of epithelial and luminal cells, while vimentin is a marker of mesenchymal cells.

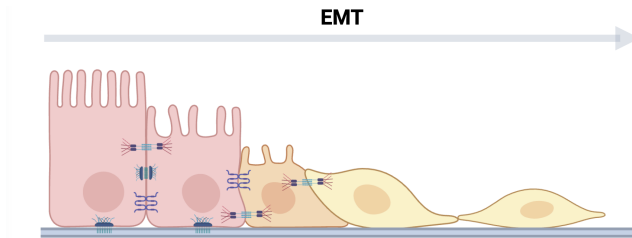


Figure 1. Illustration of epithelial to mesenchymal transition. The process by which epithelial cells lose cell-cell adhesion and develop mesenchymal features is depicted from left to right. Cells closest to the epithelial phenotype are shown in red, while cells closest to the mesenchymal phenotype are shown in yellow.

Despite existing knowledge of primary tumor subtypes, it remains unclear whether bone metastases can be categorized into subtypes that correspond to different primary tumors or if the bone microenvironment causes tumor cells to develop new features. For instance, it is unclear whether bone metastases from primary tumors with high AR expression also exhibit high AR expression, and vice versa.

To investigate these dynamics, we use genetically engineered mouse models (GEMMs) that recapitulate different phenotypes of human prostate cancer from pre-invasive to metastatic. GEMMs allow for the study of cancer progression in the context of the whole organism, and this is critical to understanding metastasis, which results from coordinated adaptive changes throughout tumor evolution (Arriaga and Abate-Shen 2019). Of particular interest to this study are the NPK (*Nkx3.1*^{CreERT2/+}; *Pten*^{flox/flox}; *Kras*^{LSL-G12D/+}; *R26R-CAG*^{LSL-EYFP/+}) and NPp53Rb1^{+/−} (*Nkx3.1*^{CreERT2/+}; *Rb1*^{flox/+}; *Pten*^{flox/flox}; *p53*^{flox/flox}; *R26R-CAG*^{LSL-EYFP/+}) genotypes. Because the *Nkx3.1* homeobox gene is primarily expressed in prostate luminal cells, an inducible Cre allele, *Nkx3.1*^{CreERT2/+}, is used for prostate-specific gene recombination. In addition, enhanced yellow fluorescent protein (EYFP) is used as a reporter allele to identify cells originating from primary tumors. The NPK genotype is further characterized by homozygous loss of function of the phosphatase and tensin homolog (*Pten*) and activation of the *Kras* oncogene, which is involved in the RAS signaling pathway. RAS signaling regulates cell growth, proliferation, and differentiation, and is significantly more altered in metastases compared to primary tumors of

human prostate cancer (Armenia *et al.* 2018). The NPp53Rb1 genotype is further characterized by heterozygous loss of function of the retinoblastoma (*Rb1*) tumor suppressor and homozygous loss of function of the *Pten* and *Tp53* tumor suppressors. Loss of function of *Pten*, *Tp53*, and *Rb1* often occurs in advanced human prostate cancer, including CRPC, small cell or neuroendocrine prostate cancer, and other metastatic phenotypes (Hamid *et al.* 2019). Previous studies of our laboratory have shown that NPK mice develop highly metastatic adenocarcinoma with approximately 40% incidence of bone metastasis (Arriaga and Abate-Shen 2019), while the recently generated NPp53Rb1 model shows approximately 60% incidence of bone metastasis (unpublished). These findings guided our selection of GEMMs to investigate the mechanisms driving prostate cancer bone metastasis.

This study will compare AR, cytokeratin, and vimentin expression across primary tumors and metastases to bone, lung, and liver in the described GEMMs to determine whether the molecular characteristics of prostate cancer cells are preserved or altered during metastasis, knowledge that is critical to developing of effective treatments for prostate cancer bone metastasis.

II. Methods

All experiments using animals were performed according to protocols approved by the Institutional Animal Care and Use Committee (IACUC) at Columbia University Medical Center. Tissue samples were acquired from three NPK (Nkx3.1^{CreERT2/+}; *Pten*^{flox/flox}; *Kras*^{LSL-G1D/+}; R26R-CAG-^{LSL-EYFP/+}) and three NPp53Rb1 (Nkx3.1^{CreERT2/+}; *Rb1*^{flox/+}; *Pten*^{flox/flox}; *p53*^{flox/flox}; R26R-CAG-^{LSL-EYFP/+}) genetically-engineered mouse models (GEMMs), which were administered tamoxifen at 2-3 months of age, monitored throughout disease progression, and ultimately euthanized by carbon dioxide inhalation once they reached the clinical endpoint. The tissues of interest for this project included primary tumors of the prostate and metastases to the bone, liver, lung, and lymph nodes. After fixation with 10% buffered formalin (soft tissues) or 4% paraformaldehyde (bones), the tissues were dehydrated, cleared, and embedded in paraffin wax using a Tanner TN1700 Embedding Center. Prior to embedding, bones were decalcified for three weeks in 15% EDTA pH 7.0 solution. A Leica HistoCore AUTOCUT Microtome was used to produce 3 μm tissue sections, which were mounted onto microscope slides. Harris Hematoxylin and Eosin (H&E) staining was performed to analyze the morphology of each sample.

Selected cases were used for immunohistochemical (IHC) analysis. After deparaffinization in xylene and citrate-based antigen retrieval, the sections were incubated overnight at 4°C with the following primary antibodies: anti-green fluorescent protein (GFP), anti-androgen receptor (AR), anti-vimentin (VIM), and anti-pan-cytokeratin (PanCK). Subsequently, the sections were incubated with secondary antibodies for 1 hour at room temperature. The Vectastain AC system and NovaRed Substrate Kit were used to develop the sections, and images were taken with an Olympus VS120 whole-slide scanning microscope. Additional probes for immunohistochemistry were identified based on results from single cell sequencing of the same mice.

III. Results

a. Prostate cancer cells retain their molecular phenotypes during metastatic progression

To investigate the molecular mechanisms of bone metastasis, we first analyzed the histopathological features of prostate tumors and their matching metastatic sites. Hematoxylin and Eosin staining was performed to visualize the morphology of each tissue. Two key biological processes that contribute to prostate cancer metastasis are androgen receptor (AR) signaling and epithelial-mesenchymal transitions (EMT). Accordingly, we evaluated the expression of AR, vimentin (VIM), and pan-cytokeratin (PanCK) in primary prostate tumors and metastases to the lung, liver, and bones in NP, NPK, and NPp53Rb1^{+/−} mouse models. Immunohistochemistry was used for qualitative analysis, where expression was noted as positive (+), low positive (low), or negative (−). In NPK and NPp53Rb1^{+/−} mice, the included regions of metastasis were positive for green fluorescent protein (GFP), confirming that the cells originated from the primary prostate tumor. Furthermore, the expression of AR, VIM, and PanCK in metastatic lesions corresponded to that in their matched primary tumors. Because metastases developed in different bones across mouse models, different skeletal sites were imaged and analyzed for each genotype. Distinct expression patterns were observed between the NPK and NPp53Rb1^{+/−} models, suggesting genotype-specific differences in tumor and metastatic phenotypes (Table 1).

Table 1. Summary of androgen receptor, vimentin, and pan-cytokeratin expression in primary tumors and metastases. The mark “low” indicates positive expression that is relatively low compared to other instances of positive expression. The data shown represents overall trends in expression for each genotype.

Genotype	Androgen Receptor (AR)				Vimentin (VIM)				Pan-Cytokeratin (PanCK)			
	Primary	Lung	Liver	Bone	Primary	Lung	Liver	Bone	Primary	Lung	Liver	Bone
NP (n=1)	+	N/A	N/A	N/A	−	N/A	N/A	N/A	+	N/A	N/A	N/A
NPK (n=3)	+	+	+	+	+	+	+	+	+	+	+	+
NPp53Rb1(+/-) (n=3)	−	−	−	−	−	−	−	−	+	+	low	+

b. Primary tumors of NP mice express AR and PanCK

In all images of immunohistochemical staining, red staining indicates positive expression of markers and blue indicates negative. Analysis of primary tumors and metastases began with identifying GFP-positive (red) regions, as these regions contain cells originating from the primary prostate tumor due to the *Nkx3.1*^{CreERT2/+} allele. Expression of AR, VIM, and PanCK was assessed only in GFP-positive regions. Non-specific staining, which refers to background staining around cells or along tissue edges, was excluded from analysis.

NP mice develop prostatic intraepithelial neoplasia (PIN) with absence of metastasis, as evidenced by the absence of positive GFP staining in lung, liver, and bone tissues. Primary tumors were positive for AR and PanCK and negative for VIM. VIM was expressed only in the prostate stroma, not in tumor cells, as regions positive for GFP were negative for VIM. Because NP mice do not form metastatic lesions, images of bone, liver, and lung tissue were taken in normal regions (Figure 2). Normal lung, liver, and bone tissues were negative for AR and

PanCK. VIM was expressed in bone marrow from normal bones but not in normal lung or liver tissues. (Figure 2).

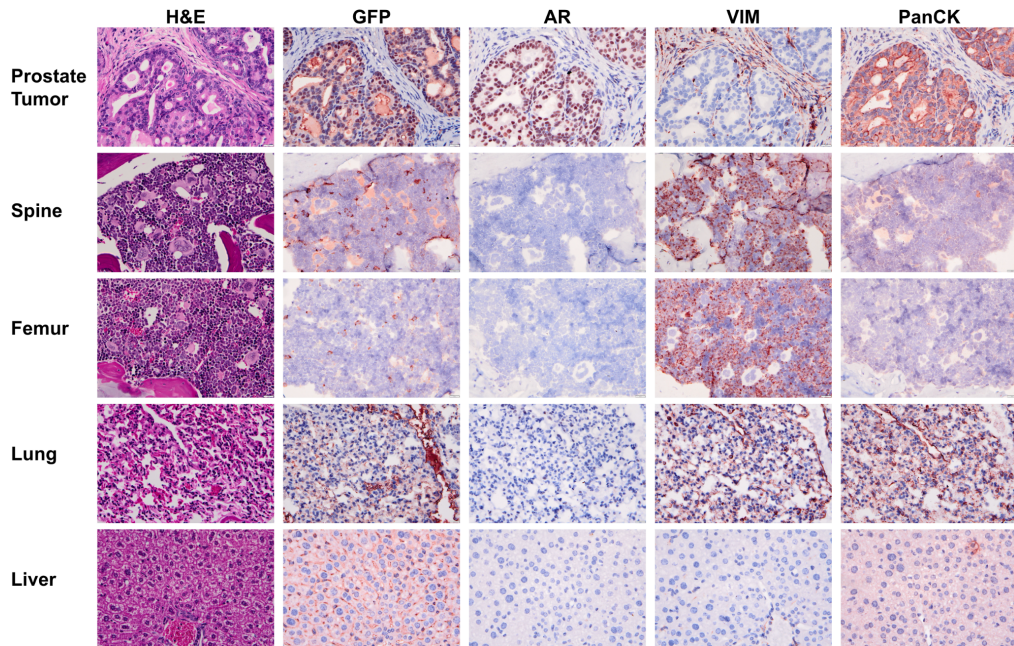


Figure 2. Histopathological analysis of prostate, bone, lung, and liver tissue from NP mice. Images were taken at 40x magnification using an Olympus VS120 whole-slide scanning microscope. Images were taken of Hematoxylin and Eosin (H&E) staining and immunohistochemistry with anti-green fluorescent protein (GFP), anti-androgen receptor (AR), anti-vimentin (VIM), and anti-pan-cytokeratin (PanCK), with positive expression shown in red.

c. *Primary tumors and metastatic lesions of NPK mice express AR, VIM, and PanCK*

For each of the NPK and NP^{p53Rb1^{+/-}} genotypes, expression patterns were summarized across three mice, and representative images were selected from a single mouse. The primary tumors of NPK mice were positive for AR, VIM, and PanCK. Lung metastases were positive for AR in two of three mice, and liver and bone metastases were positive for AR in all three mice. All sites of metastases presented positive expression of VIM and PanCK (Figure 3).

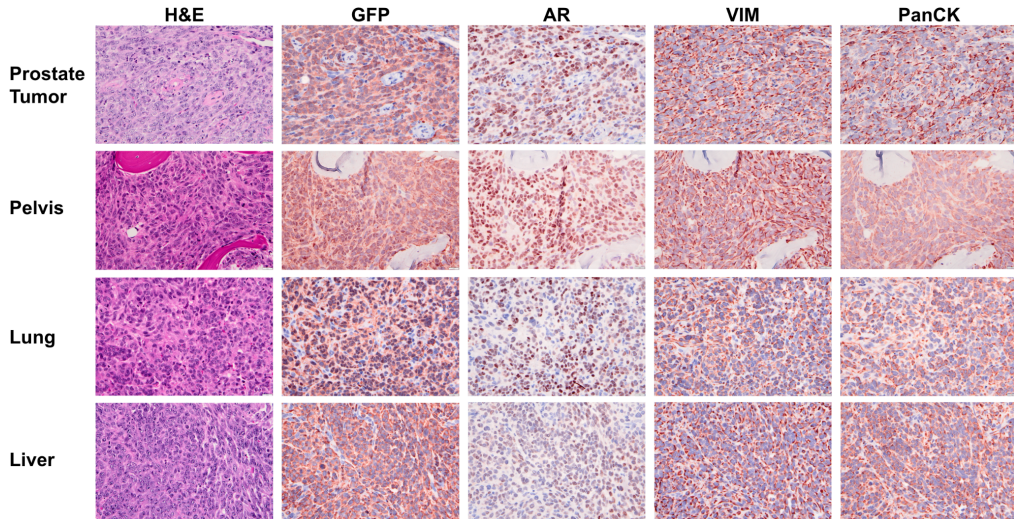


Figure 3. Histopathological analysis of prostate, bone, lung, and liver tissue from NPK mice. Images were taken at 40x magnification using an Olympus VS120 whole-slide scanning microscope. Images were taken of Hematoxylin and Eosin (H&E) staining and immunohistochemistry with anti-green fluorescent protein (GFP), anti-androgen receptor (AR), anti-vimentin (VIM), and anti-pan-cytokeratin (PanCK), with positive expression shown in red.

d. *Primary tumors and metastatic lesions of NPp53Rb1^{+/−} mice express only PanCK*

In contrast to NP and NPK mice, NPp53Rb1^{+/−} mice developed primary tumors with no AR expression in all analyzed cases. In accordance, bone and visceral metastases also presented negative AR expression. All primary tumors and sites of metastasis were negative for VIM but positive for PanCK (Figure 4).

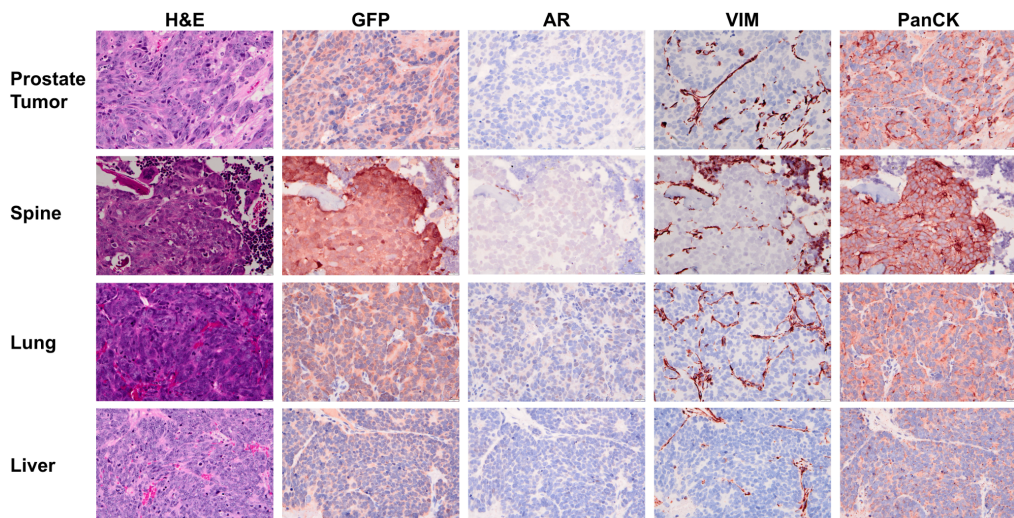


Figure 4. Histopathological analysis of prostate, bone, lung, and liver tissue from NPp53Rb1^{+/−} mice. Images were taken at 40x magnification using an Olympus VS120 whole-slide scanning microscope. Images were taken of Hematoxylin and Eosin (H&E) staining and immunohistochemistry with anti-green

fluorescent protein (GFP), anti-androgen receptor (AR), anti-vimentin (VIM), and anti-pan-cytokeratin (PanCK), with positive expression shown in red.

IV. Discussion

Histopathological analysis was performed on primary tumors and metastases to the lung, liver, and bone in NPK and NPp53Rb1^{+/−} mouse models of advanced prostate cancer. In both genotypes, expression of AR, VIM, and PanCK in metastatic sites corresponded to expression in primary tumors, suggesting that the molecular phenotype of prostate cancer cells is largely retained during metastatic progression.

Notably, the molecular phenotypes of primary tumors and bone metastases varied by genotype. In NPK mice, which are characterized by *Pten* loss of function and *Kras* activation, primary tumors and matched metastases expressed AR, VIM, and PanCK. This indicates a prostate cancer phenotype with active AR signaling and epithelial-to-mesenchymal transition. Consistent with previous studies reporting invasive adenocarcinoma in NPK mice (Arriaga and Abate-Shen 2019), H&E staining showed poorly differentiated tumor morphology. By contrast, primary tumors and matched metastases from NPp53Rb1^{+/−} mice, which are characterized by *Pten*, *Tp53*, and *Rb1* loss of function, only expressed PanCK, the epithelial and luminal cell marker, with no expression of AR or VIM. In line with these findings, previous studies have shown that joint *Pten* and *Tp53* loss of function, as in the NPp53Rb1^{+/−} genotype, results in mouse models that recapitulate neuroendocrine prostate cancer with loss of AR expression (Formaggio *et al.* 2021).

Despite differences in histological and molecular phenotype, both NPK and NPp53Rb1^{+/−} genotypes have high incidences of bone metastases, indicating that distinct mechanisms drive prostate cancer bone metastasis. In NPK tumors, bone metastases may be mediated by AR signaling and the epithelial-to-mesenchymal transition. In NPp53Rb1^{+/−} tumors, a neuroendocrine-like phenotype may develop through lineage plasticity, enabling AR-independent mechanisms of metastasis. Importantly, these different metastatic mechanisms may require fundamentally different treatment strategies in a clinical context, highlighting the importance of distinguishing prostate cancer subtypes.

As this study involved three NPK and three NPp53Rb1^{+/−} mice, additional research may involve increasing sample size to confirm the results. Furthermore, introducing androgen deprivation via surgical castration of mice could reveal the impact of AR pathway suppression on metastatic phenotype. As the findings suggest that the NPp53Rb1^{+/−} genotype may recapitulate neuroendocrine prostate cancer, immunohistochemical analysis of primary tumors and metastases could be performed with neuroendocrine markers such as ASCL1 and INSM1. Lastly, the methods of this study could be integrated with single-cell RNA sequencing to identify additional markers of interest and ex-vivo modeling to validate potential drivers of bone metastasis.

In conclusion, androgen receptor, vimentin, and cytokeratin expression in metastatic sites resembled that in primary tumors, suggesting that intrinsic tumor characteristics play a dominant role in determining the metastatic phenotype. Furthermore, the distinct expression profiles of NPK and NPp53Rb1^{+/−} mice support the existence of differing mechanisms of metastasis among prostate cancer subtypes. While current therapies for prostate cancer bone metastasis target the bone remodeling process, the findings demonstrate the need for subtype-specific approaches to better understand metastatic mechanisms and improve clinical outcomes.

V. Bibliography

1. Siegel, R. L., et al. (2025). Cancer statistics, 2025, CA: A Cancer Journal for Clinicians. **75**(1):10–45. <https://doi.org/10.3322/caac.21871>
2. Rebello, R.J., et al. (2021). Prostate cancer, Nature Reviews Disease Primers. **7**(9). <https://doi.org/10.1038/s41572-020-00243-0>
3. Arriaga, J. M., et al. (2020) A MYC and RAS co-activation signature in localized prostate cancer drives bone metastasis and castration resistance, *Nature Cancer.* **11**:1082-1096.
4. Wang, W., et al. (2019). Prostate cancer promotes a vicious cycle of bone metastasis progression through inducing osteocytes to secrete GDF15 that stimulates prostate cancer growth and invasion, *Oncogene.* **38**:4540–4559. <https://doi.org/10.1038/s41388-019-0736-3>
5. Baldessari, C., et al. (2023). Bone metastases and health in prostate cancer: From pathophysiology to clinical implications, *Cancers.* **15**(5):1518. <https://doi.org/10.3390/cancers15051518>
6. Marra, G. et al. (2023). Impact of epithelial histological types, subtypes, and growth patterns on oncological outcomes for patients with nonmetastatic prostate cancer treated with curative intent: A systematic review, *European Urology.* **84**(1):65-85. <https://doi.org/10.1016/j.eururo.2023.03.014>
7. Fujita, K. and Nonomura, N. (2019). Role of androgen receptor in prostate cancer: A review, *World Journal of Men's Health.* **37**(3):288–295. <https://doi.org/10.5534/wjmh.180040>
8. Tan, M.H.E., et al. (2015). Androgen receptor: structure, role in prostate cancer and drug discovery, *Acta Pharmacologica Sinica.* **36**:3–23.<https://doi.org/10.1038/aps.2014.18>
9. Mittal, V. (2018). Epithelial mesenchymal transition in tumor metastasis, *Annual Review of Pathology.* **24**(13):395-412. <https://doi.org/10.1146/annurev-pathol-020117-043854>
10. Arriaga, J. M. and Abate-Shen, C. (2019). Genetically-engineered mouse models of prostate cancer in the post-genomic era, *Cold Spring Harb Perspect Med.* **9**(2). <https://doi.org/10.1101/cshperspect.a030528>.
11. Hamid, A. A. et al. (2019). Compound genomic alterations of TP53, PTEN, and RB1 tumor suppressors in localized and metastatic prostate cancer, *European Urology.* **76**(1):89-97. <https://doi.org/10.1016/j.eururo.2018.11.045>
12. Armenia, J., et al. (2018). The long tail of oncogenic drivers in prostate cancer, *Nature Genetics.* **50**(5):645–651. <https://doi.org/10.1038/s41588-018-0078-z>
13. Formaggio, N., et al. (2021). Loss and revival of androgen receptor signaling in advanced prostate cancer, *Nature Oncogene.* **40**:1205-1216. <https://doi.org/10.1038/s41388-020-01598-0>